

Granular avalanches on the Moon: Mass-wasting conditions, processes and features

B. P. Kokelaar¹, R. S. Bahia², K. H. Joy², S. Viroulet³† and J. M. N. T. Gray³

¹ School of Environmental Sciences, University of Liverpool, Liverpool L69 3BX, UK

² School of Earth and Environmental Sciences, University of Manchester, Manchester M13 9PL, UK

³ School of Mathematics, University of Manchester, Manchester M13 9PL, UK

† Current address: Institut de Physique du Globe de Paris, Sorbonne Paris Cité, 75005 Paris, France

Contents of this file

Part 1: Supporting laboratory experiments

Figures S1 to S5

Part 2: Supporting lunar context

Table S1

Figures S6 to S13

Part 1: Supporting Laboratory Experiments

Introduction

Laboratory experiments reproduce key features of natural granular flows and granular segregation processes inferred for the Moon. The figures show grains with different colors to emphasize segregation or non-mixing behavior, with high-resolution imaging to allow zoom-in examination. Experimentalists, laboratory and year are given with each explanatory figure caption.

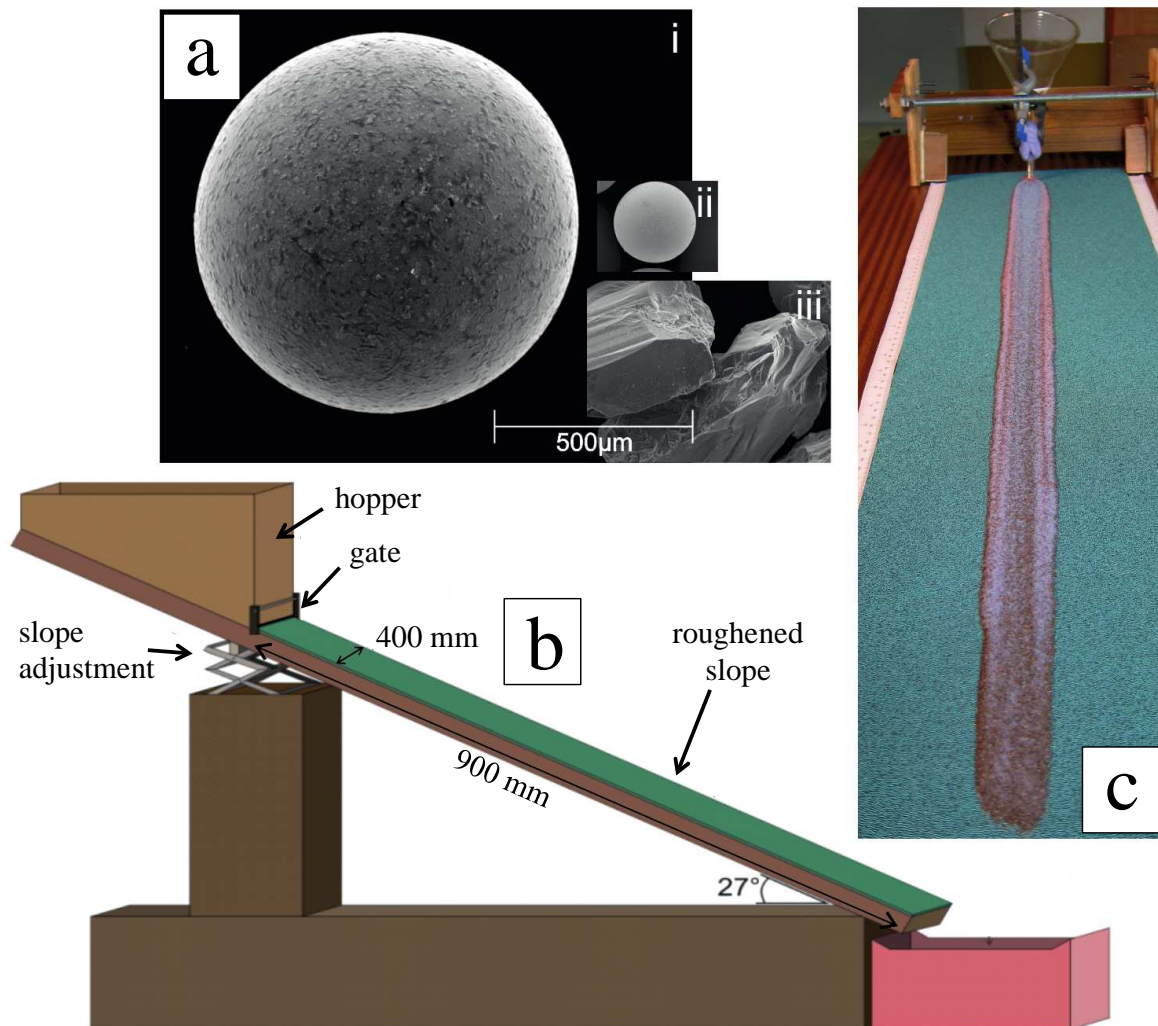


Figure S1. Small-scale granular avalanche experiment demonstrating formation of coarse-grained levees with a partly drained channel-conduit and lobate coarse-rich flow termination. a. Scanning electron microscope images of experimental particles shown at the same scale: (i) 0.75–1 mm (green) ballotini, used to roughen the slope surface; (ii) 150–250 µm ballotini (dyed red or blue) used as fine particles in experiments; (iii) 300–425 µm angular carborundum (brown). b. Experimental rig. c. Experimental runout with colour change of fine particles. A mixture of 70% fines with 30% carborundum is released steadily from a funnel 3 mm above the slope. Initial release has red fines and carborundum levees form with red fines lining. Without interrupting flow steadiness, fines are then blue and the mixture flows through the red channel-conduit to form a distal carborundum-rich lobe with blue fines in between. (Experiments by BPK, JMNTG and Romaine Graham at Liverpool, 2012.)

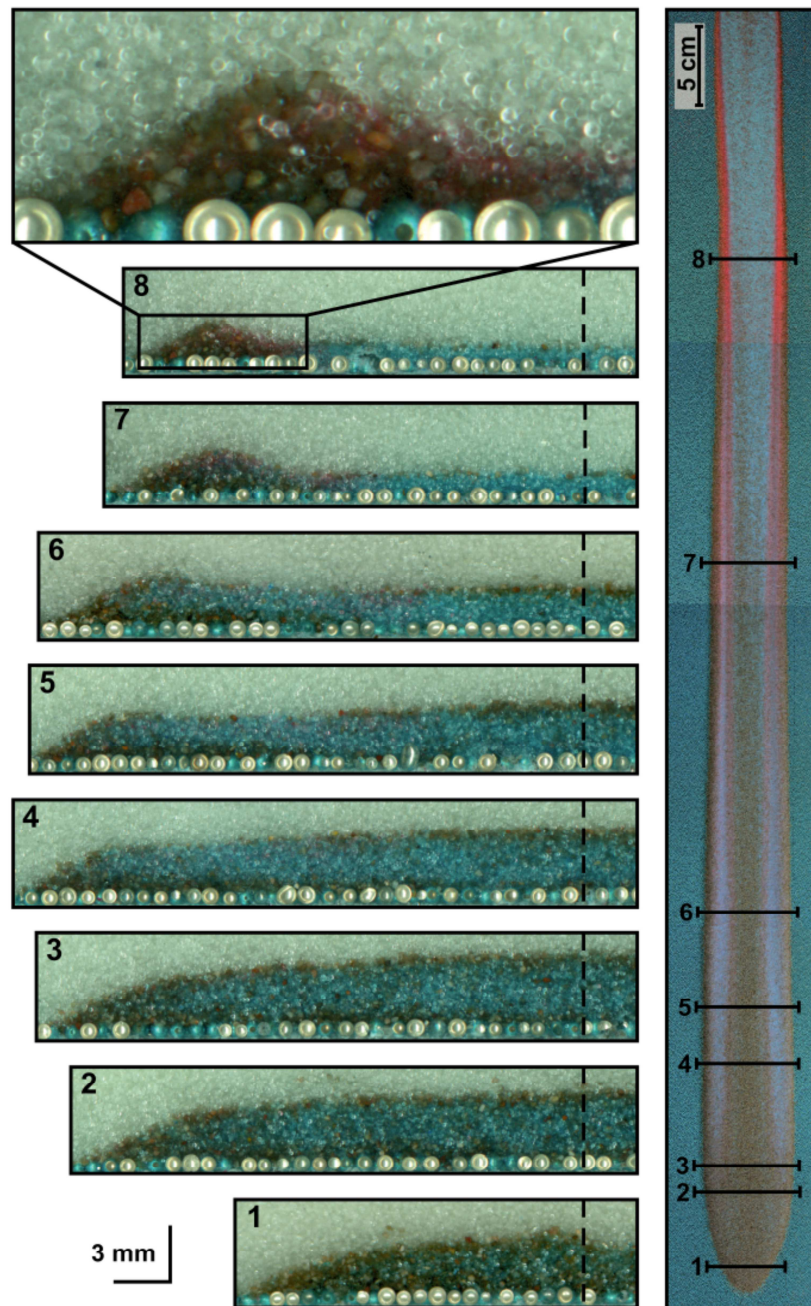


Figure S2. Experimental granular avalanche deposit similar to that shown in Figure S1. The deposit (right-hand side) is carefully buried in fine ballotini (colourless), then impregnated with colourless resin and serial sectioned. Sections are polished and scanned (sections labelled 1-8 are graphically located on the original deposit). Section 8, including enlargement, shows coarse-grained levee with red fines lining and drained channel-conduit containing blue fines and some stranded carborundum (brown). Sections 7 through to 1 show the channel-conduit with blue fines and segregated coarse carborundum on top. The lobate flow termination at sections 3-1 is coarse-rich, with carborundum on both top and base. The coarse grains have traveled to the flow front and been over-ridden; upstream such material was advected into the levees. Despite the mixture initially flowing between red fines-lined levees there are no red ballotini at the flow front, which emphasizes the efficacy of the channel-conduit. (Experiments by BPK, JMNTG and Romaine Graham at Liverpool, 2012.)

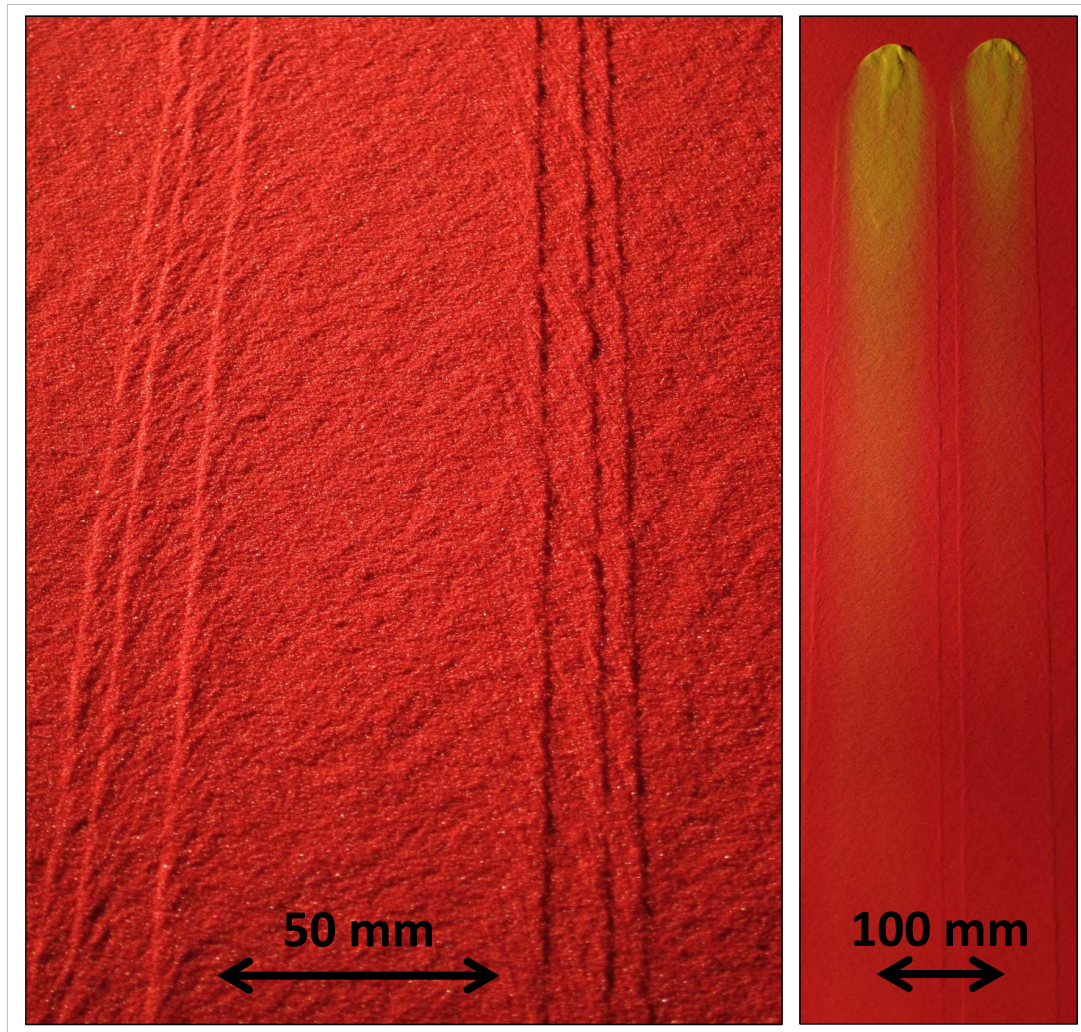


Figure S3. Experimental erosion-deposition (e-d) wave deposits. The grains are all subangular sand of a single size class, 125-200 μm , and in both panels an erodible layer close to dynamic repose angle, at $\sim 35^\circ$, forms substrate. The left panel shows the result of three successive singular releases from a small cylinder onto the slope, respectively 30, 20 and 10 ml. The tracks of the solitary e-d waves are straight and parallel sided, the levees are slightly elevated and the channel base is slightly deeper than the level of the original surface. The wave advance is steady and there is no net erosion or deposition, just reorganization. The panel on the right shows consequences of 20 ml and 10 ml releases of yellow sand. The released mass advances by erosion-deposition, gradually depositing all of the initial yellow charge so that eventually the wave propagation only involves the red slope substrate. (Experiments by SV, JMNTG, BPK and James Vallance at Manchester, 2016.)

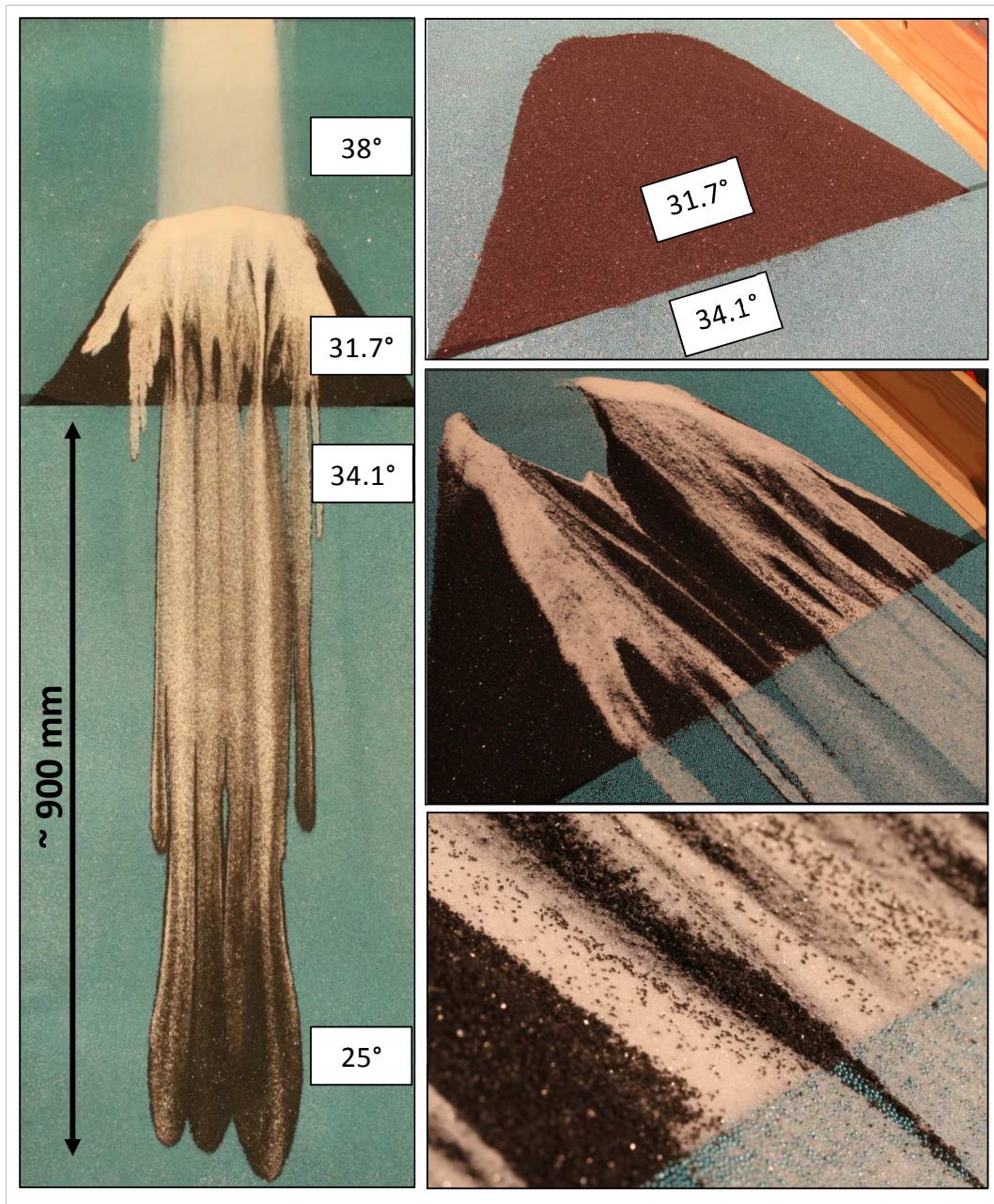


Figure S4. Experiment demonstrating mobilization of stable coarse material by inundation with fines. Left-hand panel is overhead view of experiment in progress. The black grains are sand resting stably close to the dynamic repose angle on a narrow ledge that crosses the experimental slope. This pile was formed by pouring the sand (300–600 μm) across the ledge to form a dynamic repose-angled slope-wedge, at $\sim 31.7^\circ$. Fine white ballotini (75–150 μm) were then released from a hopper at the top of the slope, which was much steeper (38°) than their dynamic repose angle ($\sim 23.1^\circ$). As the fines inundate the coarse deposit the mixture is mobilized and continues in several streams downslope, segregating to form coarse levees and distal coarse-rich lobes. The lowermost ~ 450 mm of the slope was gradually curved to lesser angles (25 - 20°) to promote deposition. Downwards tapering coarse streaks extend from the edge of the ledge. (Experiments by BPK, SV and JMNTG at Manchester, 2016.)

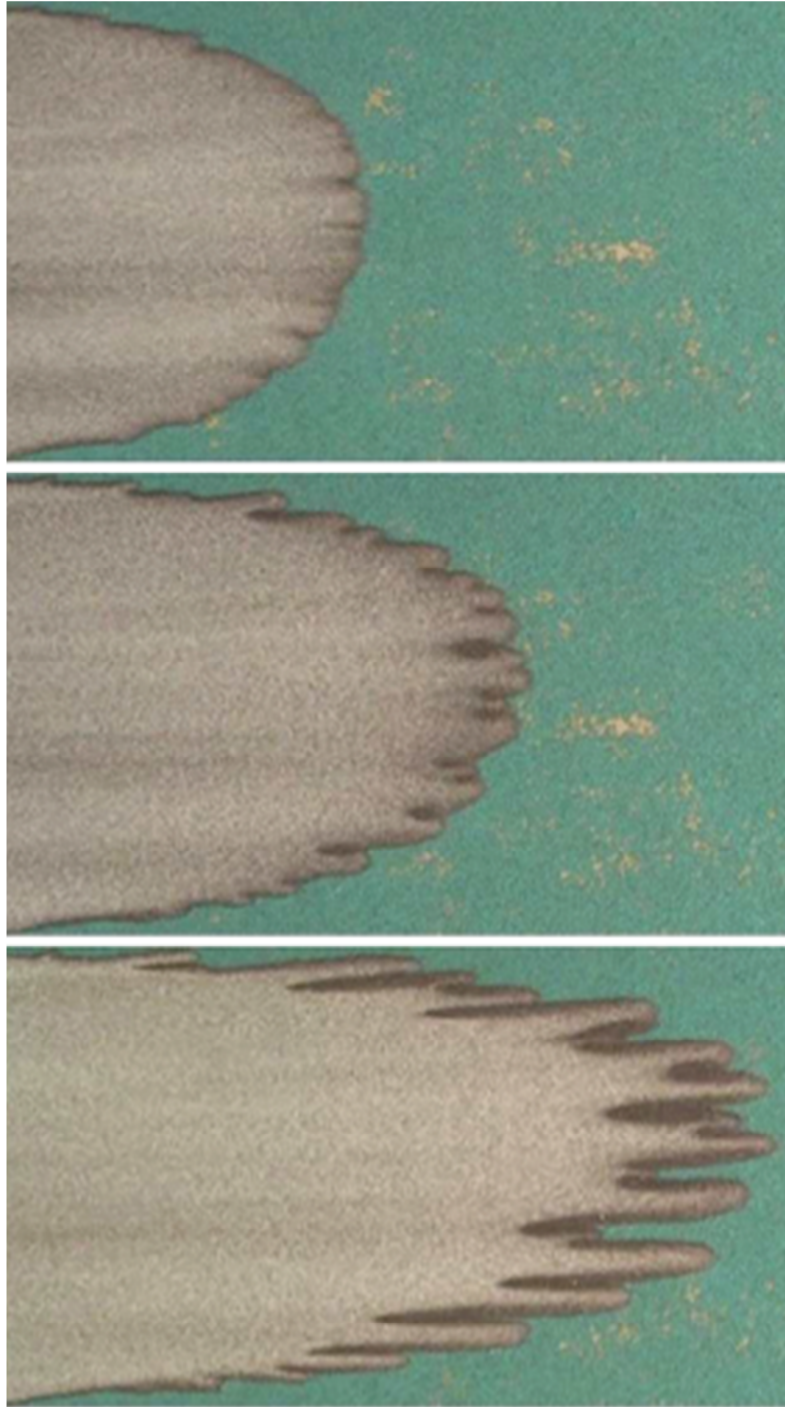


Figure S5. Overhead views of an experiment in which a mixture of spherical (white) glass ballotini (75–150 μm ; 70%) and angular-irregular (brown) carborundum grains (315–350 μm ; 30%) is released from a linear hopper onto a plane slope at 27° . The slope is roughened with a monolayer of (green) glass ballotini (0.75–1 mm). Size segregation concentrates coarse particles on the flow top and velocity shear through the avalanche preferentially transports these towards the flow front, where they may be overrun and segregate to the surface again. The accumulation of the larger more resistive grains at the flow front first leads to a crudely periodic lateral instability, from which the front then degenerates into a series of lobes and then growing distinct fingers with coarse-grained margins. The images are approximately $0.5\text{ m} \times 0.3\text{ m}$. (Experiments by Mark Woodhouse, JMNTG and BPK at Manchester, 2011.)

Part 2: Supporting lunar context

Table S1. Details of resolution and phase angle of images used in this study.

LROC Image Identifier	Image Site	Mean Resolution (m)	Phase Angle (Max/Min)
M133078533LE	Kepler	0.462	69.94 / 67.04
M173165404RE	Kepler	0.425	21.27 / 18.29
M1129731152LE	Kepler	1.068	45.73 / 42.67
M135263529RE	Gambart B	0.485	59.05 / 56.13
M135073175RE	Bessel	0.468	64.24 / 61.22
M1151745229RE	Bessel	1.259	44.19 / 40.69
M139694087RE	Censorinus	0.488	9.67 / 6.70
M112074670RE	Riccioli CA	0.485	34.24 / 31.30
M167043682RE	Virtanen F	0.622	43.27 / 40.20
M169398317RE	Virtanen F	0.422	30.30 / 27.36
M111286669RE	Tralles A	0.472	37.95 / 35.67
M1123292388RE	Tralles A	1.341	68.08 / 64.82
Lunar LRO LROC-WAC Mosaic global 100 m	All	100.0	N/A

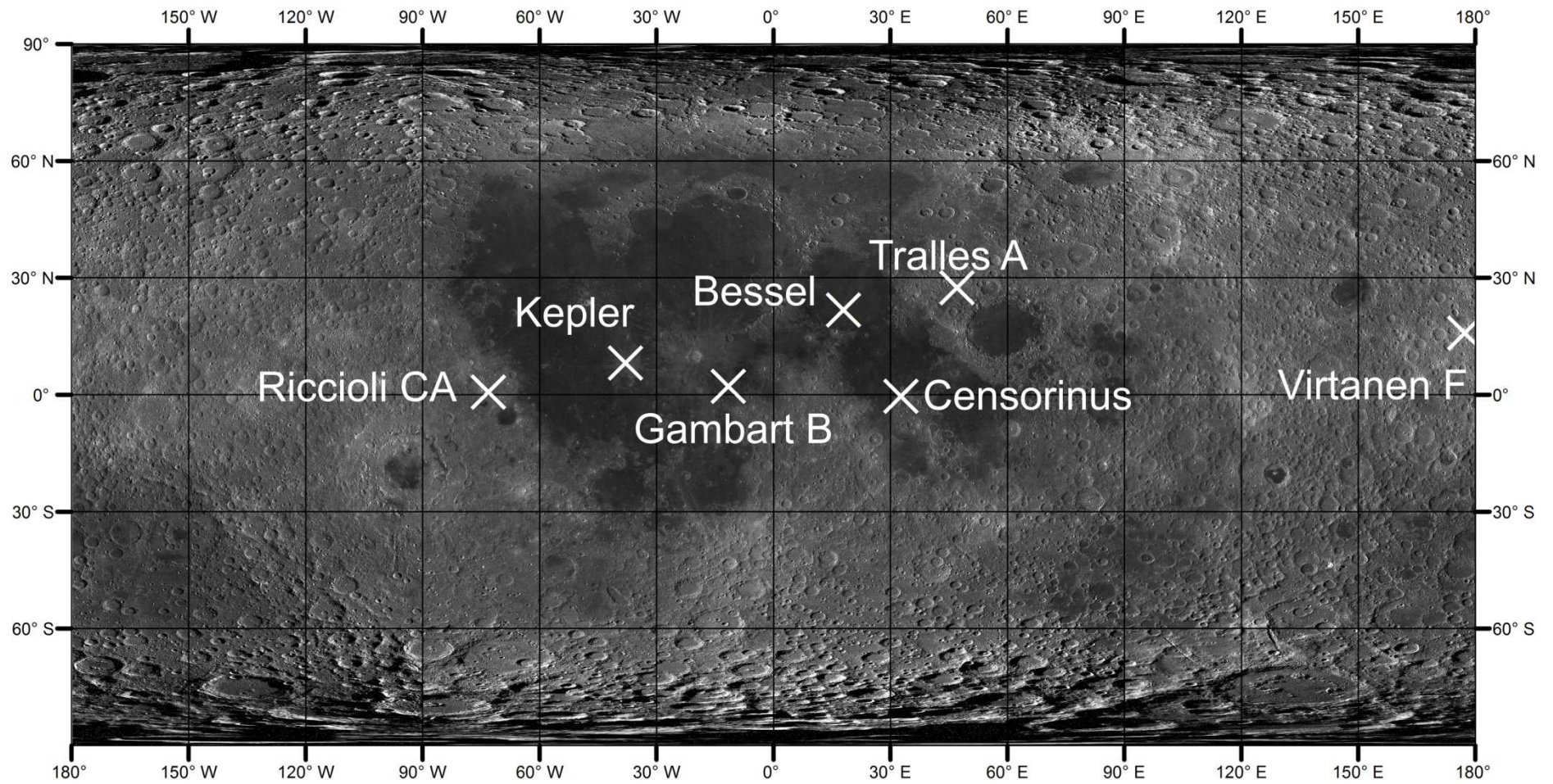


Figure S6. Context image depicting the location of all sites investigated. Lunar LRO LROC-WAC Mosaic global 100 m image courtesy of NASA/GSFC/ASU.

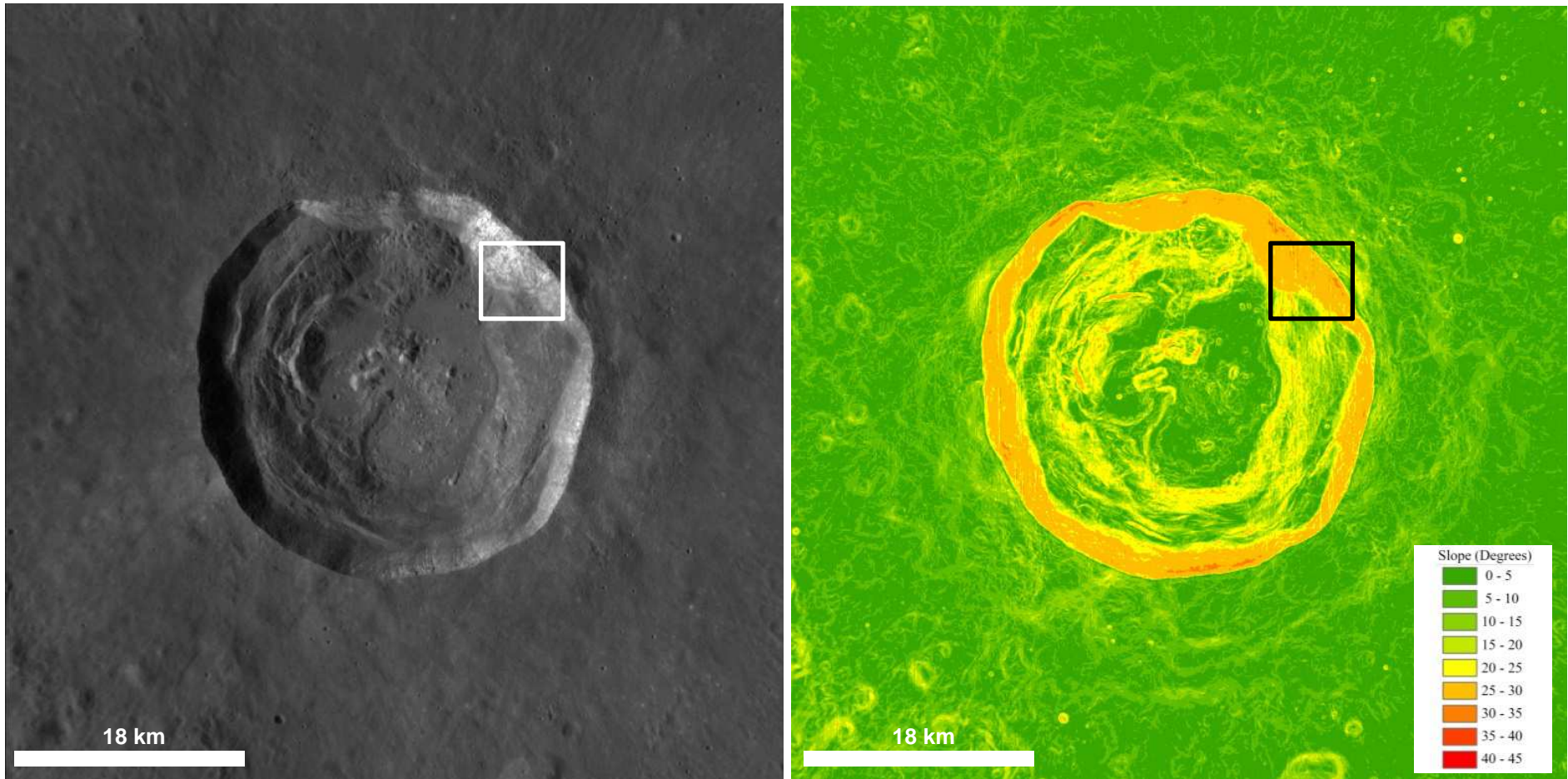


Figure S7. Kepler site context image (a), with slope image (b). The boxes in panels (a) and (b) show the study site location. LRO LROC-WAC Mosaic global 100 m courtesy of NASA/GSFC/ASU.

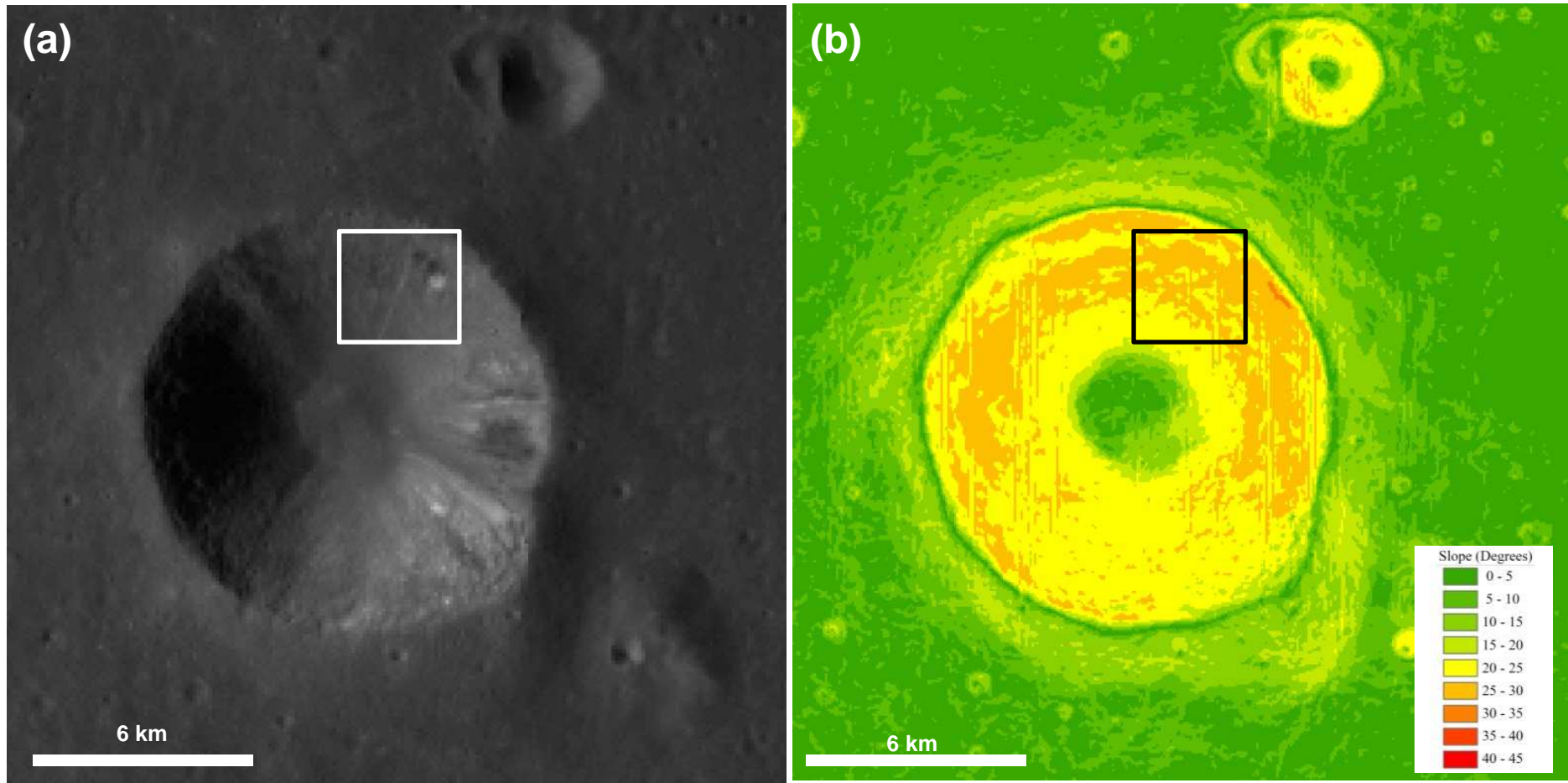


Figure S8. Gambart B site context image (a), with slope image (b). The boxes in panels (a) and (b) show the avalanche site location. Lunar LRO LROC-WAC Mosaic global 100 m image courtesy of NASA/GSFC/ASU.

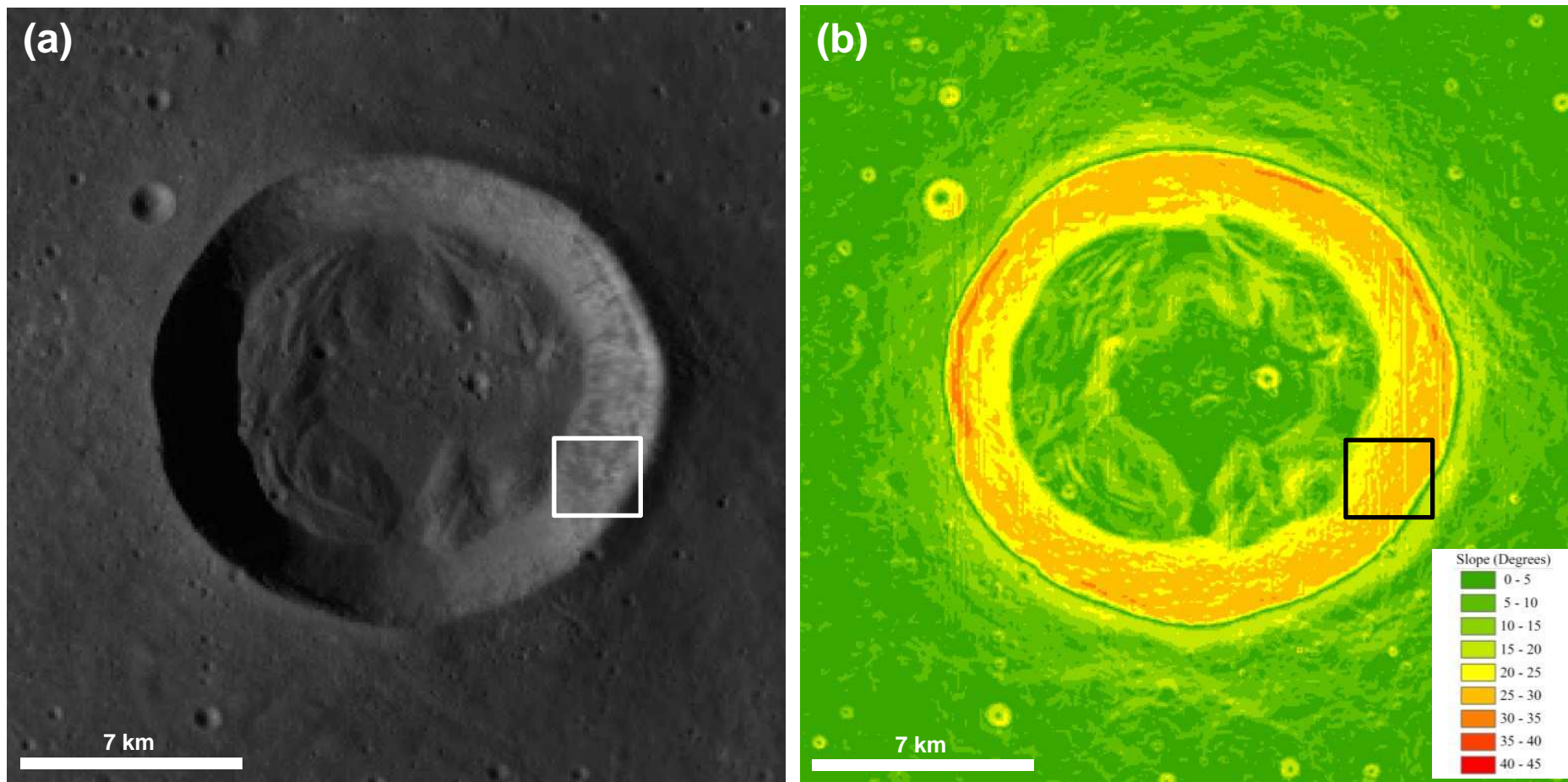


Figure S9. Bessel site context image (a), with slope image (b). The boxes in panels (a) and (b) show the avalanche site location. Lunar LRO LROC-WAC Mosaic global 100 m image courtesy of NASA/GSFC/ASU.

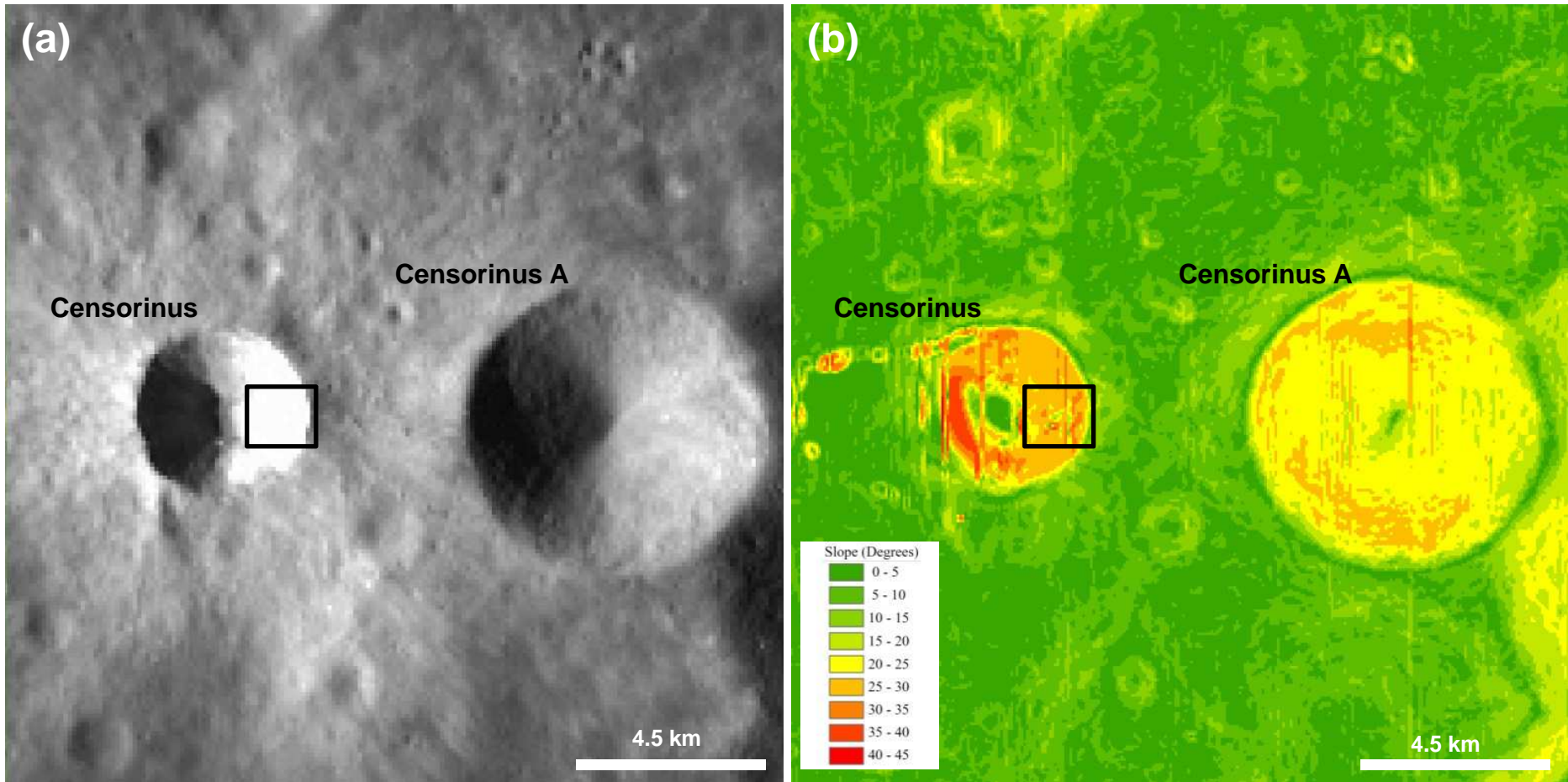


Figure S10. Censorinus site context image (a), with slope image (b). The boxes in panels (a) and (b) show the avalanche site location. Lunar LRO LROC-WAC Mosaic global 100 m image courtesy of NASA/GSFC/ASU.

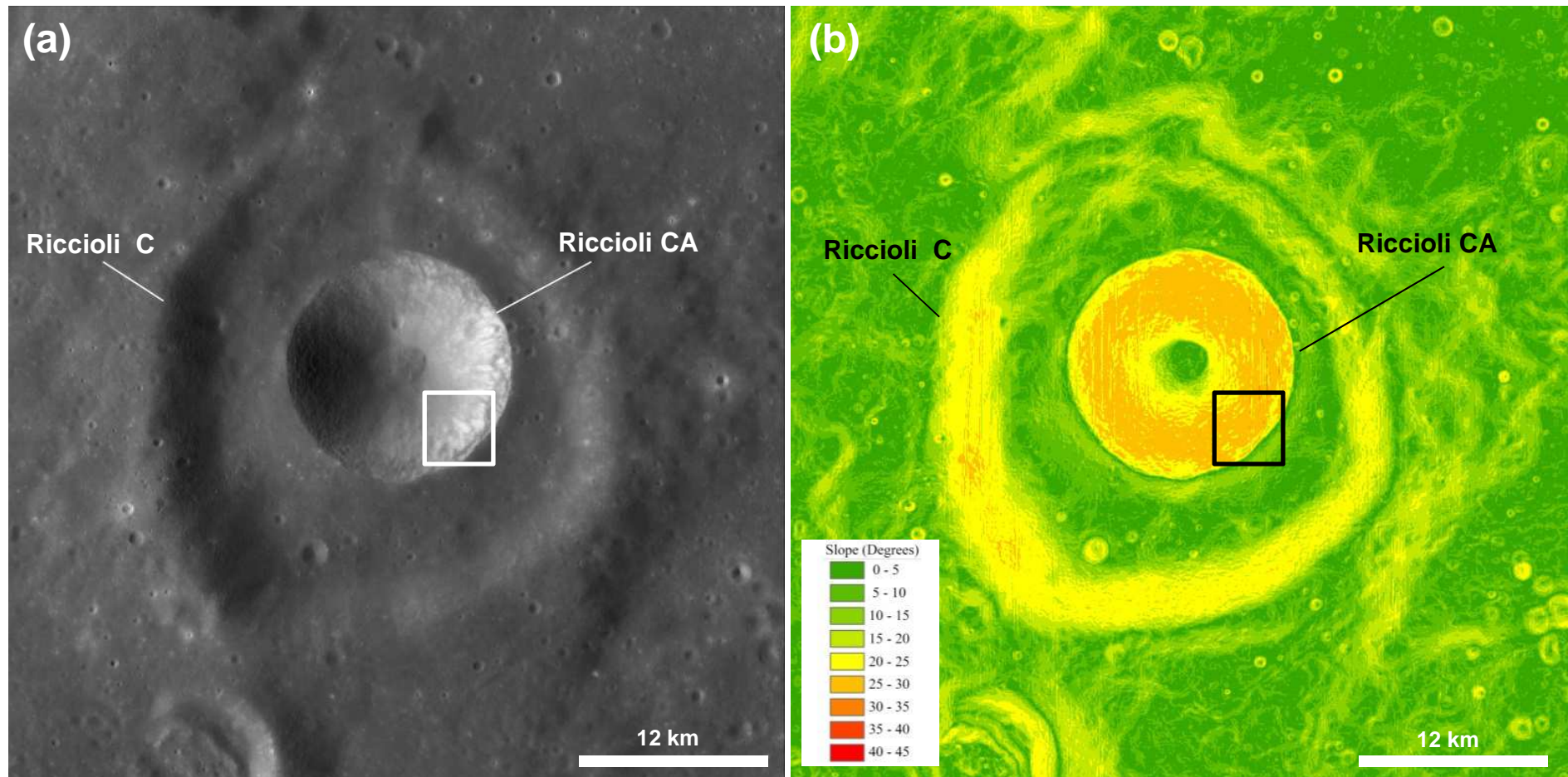


Figure S11. Riccioli C site context image (a), with slope image (b). The boxes in panels (a) and (b) show the avalanche site location. Lunar LRO LROC-WAC Mosaic global 100 m image courtesy of NASA/GSFC/ASU.

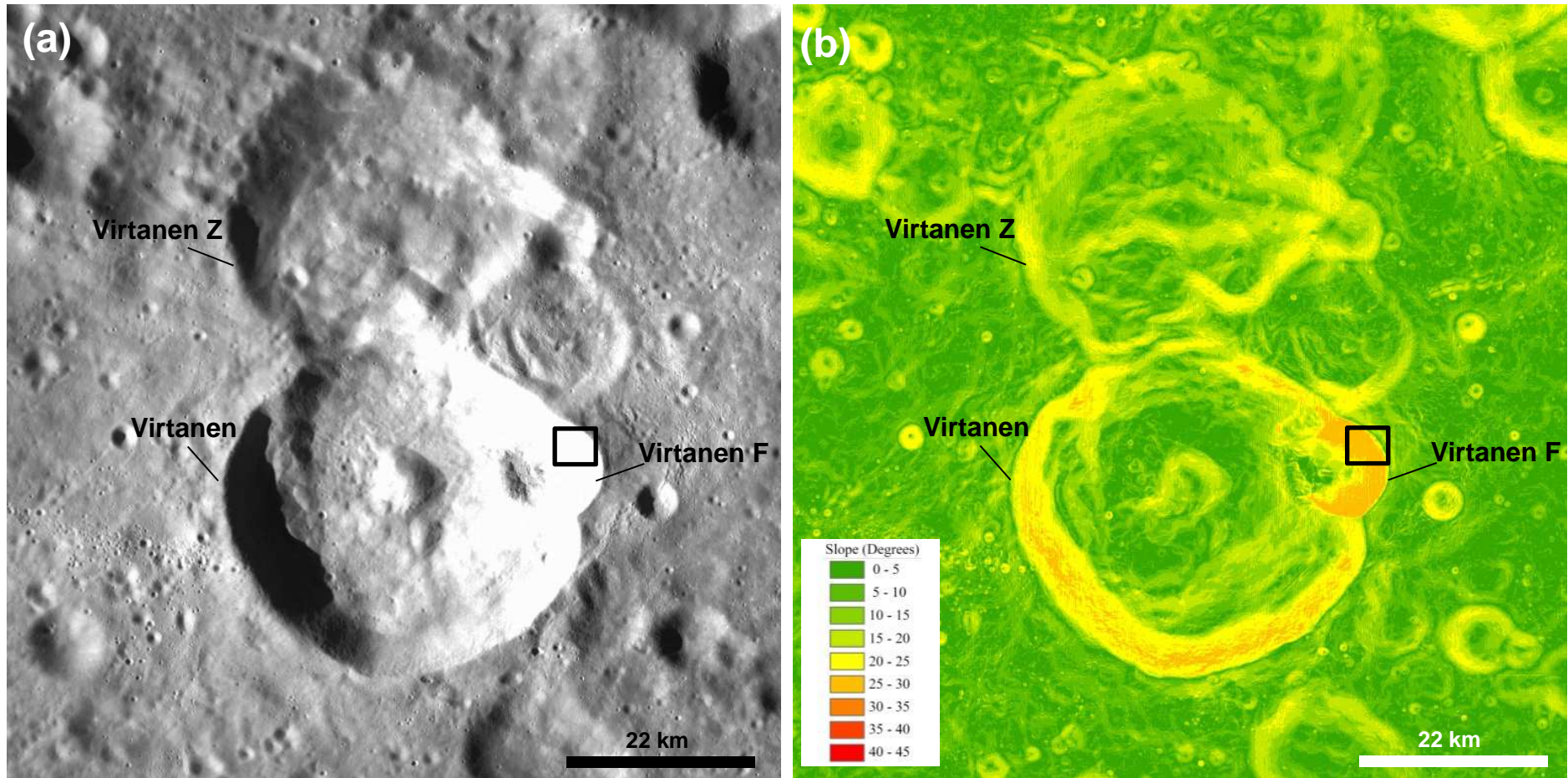


Figure S12. Virtanen F site context image (a), with slope image (b). The boxes in panels (a) and (b) show the avalanche site location. Lunar LRO LROC-WAC Mosaic global 100 m image courtesy of NASA/GSFC/ASU.

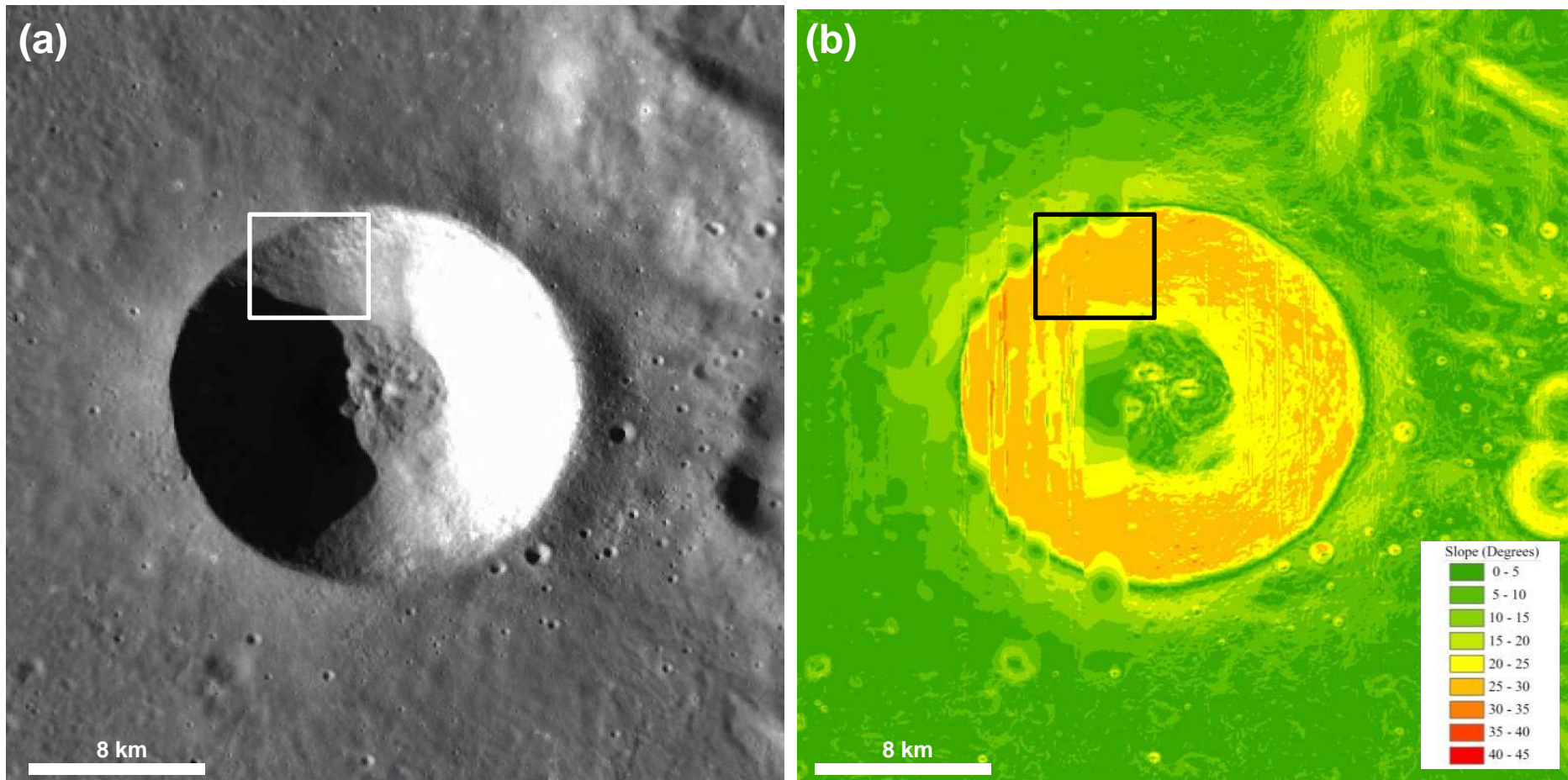


Figure S13. Tralles A site context image (a), with slope image (b). The boxes in panels (a) and (b) show the avalanche site location. Lunar LRO LROC-WAC Mosaic global 100 m image courtesy of NASA/GSFC/ASU.